eSim 2018
«BUILDING SIMULATION TO SUPPORT BUILDING SUSTAINABILITY»
IBPSA Canada
The Canadian Chapter of the International Building Performance Simulation Association
Le chapitre canadien de International Building Performance Simulation Association

# Validation of RC Building Models for Applications in Energy and Demand Side Management

Ryuta Kuniyoshi[1], Michael Kramer[2], Manuel Lindauer[2]

[1] The University of Tokyo, Tokyo, Japan
[2] Technical University of Munich, Munich, Germany

***Abstract:*** *Low-order building models are widely suggested for district thermal simulations because of their low computational costs. However, low-order modelling including radiative heating systems is not yet well established. Hence, this paper investigates the accuracy of low-order resistance and capacitance (RC) models for applications in energy and demand side management. Simulations are carried out for single-family houses equipped with underfloor heating systems. A detailed reference model is created in EnergyPlus for comparison, while the RC model is based on previous literature and parameterized based on a typology approach. The analysis studies the dynamic behaviour of the indoor temperature and energy demand during a winter period. The results reveal that the modelling approach for the heating system and solar radiation limits the accuracy of the RC model. Therefore, model modification by changing relevant parameters with curve fitting techniques and by extensions of the model structure. As a result, this paper clarifies that the RC models have sufficient accuracy after the modifications.*

***Keywords:*** *RC building models, EnergyPlus, typology approach, demand side management, underfloor heating systems*

## INTRODUCTION

Demand side management (DSM) allows to use flexibility offered from heat storages in buildings for operational measures at district or urban scale level. Since a detailed thermal model and parameterization for each building is not practical from a perspective of operators or aggregators, the following two approaches are suggested in general to determine and parameterize a model structure. One approach is statistical parameter fitting using substantial amounts of measurement data. While this statistical method can identify parameters without physical information of building materials, the obtained parameters do not necessarily represent physical properties, which leads to difficulties in analysing results from a physical point of view (Reynders et al. (2014)). The other approach is to derive physical properties based on typology data. Reynders et al. (2014) and Kramer et al. (2017) identify model parameters from representative building data offered by the European research project Typology Approach for Building Stock Energy Assessment (TABULA) and establish feasible ways to create models for thermal building simulations. In these studies, models are represented by thermal resistances and capacitances (RC model) described by differential equations. Whereas RC models are evidently useful for district simulations owing to their low computational costs, nevertheless, a good trade-off between computational costs and accuracy should be aimed for. In particular, a careful analysis is necessary regarding radiation heat transfer modelling for solar radiation and radiative heating systems, since RC models usually linearize the non-linear radiative heat transfer equations for simplicity.

Hence, this paper validates the RC models with a special focus on radiative effects from solar radiation and underfloor heating systems.

## METHOD

To evaluate the accuracy of RC models, this study uses the RC models proposed by Kramer et al. (2017), which are developed based on the guideline VDI 6007. Also, detailed models are created as reference models in the transient thermal simulation program, EnergyPlus. Geometry and physical properties of the buildings are taken from available data of the TABULA typology. The TABULA Web Tool covers a large number of residential building types in European countries depending on age classes, where further distinctions are applied between single-family, multi-family, terraced houses and apartment buildings. Among various datasets, this paper focuses on single-family houses in Germany as representative cases for comparison. Weather data in Munich which is also required for the simulation is obtained in EnergyPlus weather format.

Firstly, comparisons are implemented under the assumption that the buildings do not obtain any energy from the sun and heating systems in order to reduce the complexity of thermal behaviour. The indoor temperature of a building is calculated in both the RC model and the


ISBN 978-2-921145-88-6

reference model. This comparison allows to evaluate the thermal behaviour of the building that is only dependent on convective and conductive heat transfer between ambient air and the buildings.

Subsequently, the comprehensive building models with effects of solar radiation, ventilation and thermal bridges are analysed. In order to describe the distribution of heat gains and of solar radiation on the internal building surfaces accurately, a modification of the model parameters via curve fitting leads to a more accurate (thermal) model.

Finally, the effect of a heating system is investigated. In this comparison, not only the indoor temperature but also the total energy demand is calculated as a result of an optimization problem. A statistical modification of model parameters representing the effects of the heating systems is carried out in the same manner as the modification for solar radiation to consider the heat gain from the heating system accurately. Also, a physical modification is attempted by creating an additional model component representing the long-wave radiation exchange between the building components.

# INPUT DATA

## Weather data

EnergyPlus weather format provides weather data for more than two thousand locations mainly in the USA. This study refers to the data which correspond to a weather station in Munich. The principal weather data used as inputs are ambient temperature $T_a$, ground temperature $T_g$ and solar radiation $I$. Whereas $T_a$ and $I$ are obtained from EnergyPlus weather format, $T_g$ is assumed to have a constant value of 10 °C. In EnergyPlus, the default value of the ground temperature is 18 °C, independently of the weather station. However, $T_g$ is set at 10 °C as suggested by Lindauer (2017).

## Building data

The same model structure and parameters are used as those proposed by Kramer et al. (2017) for comparability. Geometric data is necessary for parameterization and model structure. This typology approach enables a representative thermal simulation without the need of detailed information on existing buildings.

In this paper, single-family houses (SFHs) are selected for the comparison, since they are predominant in suburban and rural areas, where the transport capacity of electricity grids is often limited and thus demand side management and efficient operation of electricity consumers is of great interest and value (ZVEI et al. (2012)).

According to Kramer et al. (2017), four building types depending on age classes were identified for applications of DSM. In particular, this paper selects two building types for comparisons, Building type J and L. Those typology cases are associated with official regulations from the German Energy Saving Ordinance (EnEV), which defines minimum requirements for energy efficiency of buildings in Germany.

Building type J describes SFHs constructed during the years 2002 to 2009, just after the EnEV's first issue in 2002. Building type L represents the latest SFHs which are furnished with high-performance insulation and a heat recovery system. Further details of the two building types are summarized in Table 1. The areas of the building components, the U-values of the thermal bridges $U_{thermal\ bridge}$, the coefficients for ventilation and infiltration systems $\eta_{vent}, \eta_{inf}, \eta_{mec}, \varepsilon$ (Nielsen (2005)), are specified and discussed in the following section.

*Table 1 Geometry and parameters of the two building types*

| **Building type** | | **J** | **L** |
|---|---|---|---|
| Area [m²] | Outer wall | 188.9 | |
| | Inner wall | 188.9 | |
| | Floor | 79.8 | |
| | Roof | 85.9 | |
| | Window(N/S/E/W) | 3.1/17.3/3.9/3.9 | |
| | Door | 2 | |
| U-value of the thermal bridges $U_{thermal\ bridge}$ [W/m²K] | | 0.05 | 0.02 |
| Change rates for natural ventilation and infiltration $\eta_{vent} + \eta_{inf}$ [1/h] | | 0.5 | - |
| Change rate for mechanical ventilation $\eta_{mec}$ [1/h] | | - | 0.55 |
| Efficiency of heat recovery (mechanical ventilation) $\varepsilon$ [-] | | - | 0.84 |
| G-value of window [W/m²K] | | 0.6 | 0.6 |
| U-value of window [W/m²K] | | 0.7 | 1.4 |

Material properties of each building component such as walls, floor, roof and windows are also used as input. The prerequisite properties are the material density $\rho$, specific heat capacity $c$, conductivity $\lambda$ and thickness $s$. Because the TABULA typology does not cover all the materials and parameters that compose the building's fabric, data from


ISBN 978-2-921145-88-6

Arold (2014), Tenbohlen et al. (2015) and the ISO 10456 (2007) are used.

g- and U-values are used instead for windows. The g-value represents the permeability of solar radiation. The U-value represents the rate of heat loss through a window due to the heat transfer such as heat conduction, heat convection and heat radiation. Besides, the U-value also includes the heat loss through frames of the window.

Furthermore, the R-value is calculated from thermal properties of materials, which is used as thermal resistance R of the RC model in this paper. The R-value can evaluate the ability of a material to prevent the passage of heat. The total R-value per square meter of a component with multiple layers (v=1,…,n) is calculated by (1) in m²K/W.

$$\boldsymbol{R_{total}} = \sum_v \frac{\boldsymbol{s_v}}{\boldsymbol{\lambda_v}} \tag{1}$$

# RC MODELS

## Modelling method

With the building data mentioned in the previous section, RC models are created in the next step. RC models are composed of thermal resistances R and heat capacitances C by following the analogies of electrical circuit systems. Different RC models have been developed to simulate the thermal behaviour of buildings and the German guideline VDI 6007 describes a method for the component wise calculation.

According to VDI 6007, every component is basically represented by the 3R2C model (see Figure 1), and further reductions are possible in most cases. For example, outer walls, which have asymmetrical thermal loads on external and internal surfaces, can be represented by a 2R1C model. On the other hand, inner walls, where the two surfaces are assumed to have the same thermal loads, can be represented by a 1R1C model.

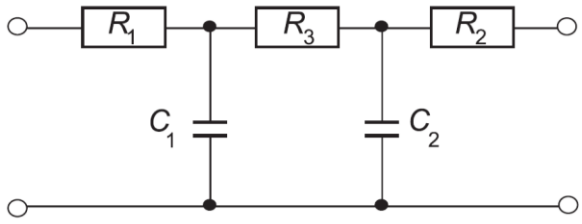


*Figure 1 3R2C model from VDI 6007*

Whereas the 2R1C model is composed of $R_1$, $R_2$ and $C_{1;korr}$, the 1R1C model is composed of $R_1$ and $C_{1;korr}$. These parameters are calculated by means of a matrix calculus approach as follows. For a homogeneous wall layer, the one-dimensional thermal behaviour can be calculated by (2),

$$\begin{pmatrix} \underline{\boldsymbol{\vartheta}}(\boldsymbol{x}=\boldsymbol{0}) \\ \underline{\boldsymbol{q}}(\boldsymbol{x}=\boldsymbol{0}) \end{pmatrix} = \boldsymbol{A_{chain}} \begin{pmatrix} \underline{\boldsymbol{\vartheta}}(\boldsymbol{x}) \\ \underline{\boldsymbol{q}}(\boldsymbol{x}) \end{pmatrix}, \tag{2}$$

where $\underline{q}$ represnts the heat flow and $\underline{\vartheta}$ represents the temperature for a coordinate x perpendicular to the wall. The chain matrix $\boldsymbol{A_{chain}}$ has four complex elements $\underline{a}_{11}, \underline{a}_{12}, \underline{a}_{21}, \underline{a}_{22}$, which are calculated from thermal resistance $R_{total}$ and heat capacitance $C_{total}$ of the layer. Details on the derivation can be found in the guideline VDI 6007. Whereas $R_{total}$ is calculated from (1), $C_{total}$ is calculated as follows with thermal storage capacity $c \cdot \rho$ [J/m³K] and thickness $s$ [m] of the layer.

$$\boldsymbol{C_{total}} = \boldsymbol{c \cdot \rho \cdot s} \tag{3}$$

In the case that a wall has multiple layers ($v = 1, \dots, n$), the whole thermal behaviour can be calculated by replacing $\boldsymbol{A_{chain}}$ in (2) with $A_1 \cdot A_2 \cdot \dots \cdot A_{n-1} \cdot A_n$ as described in (4).

$$\begin{pmatrix} \underline{\boldsymbol{\vartheta}}(\boldsymbol{x}=\boldsymbol{0}) \\ \underline{\boldsymbol{q}}(\boldsymbol{x}=\boldsymbol{0}) \end{pmatrix} = \boldsymbol{A_1 \cdot A_2 \cdot \dots \cdot A_{n-1} \cdot A_n} \begin{pmatrix} \underline{\boldsymbol{\vartheta}}(\boldsymbol{x}) \\ \underline{\boldsymbol{q}}(\boldsymbol{x}) \end{pmatrix} \tag{4}$$

As a result, $R_1, R_2$ and $C_{1;korr}$ are derived as (5) to (7) describes,

$$\boldsymbol{R_1} = \frac{\boldsymbol{1}}{\boldsymbol{A}} \frac{\left(\boldsymbol{Re\underline{a}_{22}} - \boldsymbol{1}\right) \cdot \boldsymbol{Re\underline{a}_{12}} + \boldsymbol{Im\underline{a}_{22}} \cdot \boldsymbol{Im\underline{a}_{12}}}{\left(\boldsymbol{Re\underline{a}_{22}} - \boldsymbol{1}\right)^2 + \boldsymbol{Im\underline{a}_{22}}^2}, \tag{5}$$

$$\boldsymbol{R_2} = \boldsymbol{R_{total}} - \boldsymbol{R_1}, \tag{6}$$

$$\boldsymbol{C_{1;korr}} = \boldsymbol{A} \frac{\boldsymbol{1}}{\boldsymbol{\omega_{BT} R_1 A}} \cdot \frac{\boldsymbol{R_{total} A} - \boldsymbol{Re\underline{a}_{12}} \cdot \boldsymbol{Re\underline{a}_{22}} - \boldsymbol{Im\underline{a}_{12}} \cdot \boldsymbol{Im\underline{a}_{22}}}{\boldsymbol{Re\underline{a}_{22}} \cdot \boldsymbol{Im\underline{a}_{12}} - \boldsymbol{Re\underline{a}_{12}} \cdot \boldsymbol{Im\underline{a}_{22}}}, \tag{7}$$

where A is surface area of the layer [m²] and $\omega_{BT}$ is angular frequency for the layer. In addition, thermal resistances for convection and radiation are taken into account separately. Those resistances are calculated from the convective coefficient $\alpha_{con}$ and the radiant coefficient $\alpha_{rad}$ as described in Equation (8) and (9). These resistances are connected to the resistances of components in series.

$$\boldsymbol{R_{con}} = \frac{\boldsymbol{1}}{\boldsymbol{\alpha_{con} \cdot A}} \tag{8}$$

$$\boldsymbol{R_{rad}} = \frac{\boldsymbol{1}}{\boldsymbol{\alpha_{rad} \cdot A}} \tag{9}$$

Although coefficients for convection are not constant and influenced mainly by the velocity of the air, an external convective coefficient of 20 W/(m²K) and an internal convective coefficient of 2.7 W/(m²K) are widely adopted (VDI6007 (2015) and Lauster et al. (2014)). The coefficient for radiation exchanges among the internal surfaces is also


ISBN 978-2-921145-88-6

not constant because the amount of radiation heat is proportional to the forth power of the temperature difference between two surfaces exchanging heat. Nevertheless, assuming a constant value of 5.0 W/(m²K) as $\alpha_{rad}$ is reasonable according to VDI6007. This paper follows these assumptions.

## The 6R4C model

The RC model analysed in this paper is shown in Figure 2. In contrast to the VDI 6007, which proposes a whole building model with two states representing two temperatures, the model in Figure 2 has four states representing temperatures of the zone air, the inner walls, the outer components and the floor. All thermal resistances and the indexes of the components and distribution factors are described in Table 2.

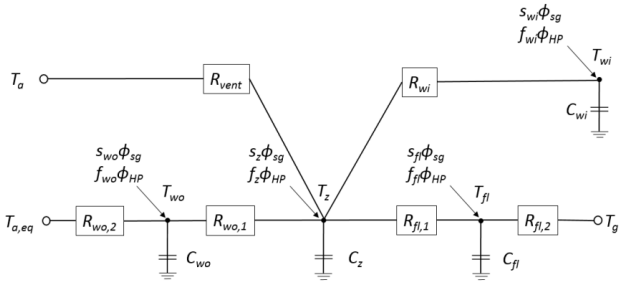


*Figure 2 The 6R4C model*

Regarding the heat exchanges which occur inside the building, the gains from solar radiation transmitted through windows and the heating system need to be considered. They are absorbed by $T_z$, $T_{wi}$, $T_{wo}$, and $T_{fl}$ based on distribution factors in the 6R4C model. First, the convective parts of those gains are separated and added to the zone air by means of the ratios such as $s_z$ and $f_z$. Those ratios are generally specified in standard guidelines. For instance, the convective part of the total solar gains ($s_z$) is assumed to be 9% (ISO13790 (2008)), the convective gains from an underfloor heating system ($f_z$) is assumed to be 5% (Ingenieurbüro für Haustechnik Schreiner (2011)). Second, the remaining parts are regarded as radiant parts and split up based on area-weighted distribution factors, which are absorbed by the internal surfaces of the components (Kramer et al. (2017)).

The internal heat exchanges between internal surfaces of building components have also influence on thermal behaviour of buildings, which occur in the form of long-wave radiation. Nevertheless, these effects are relatively small and are not described in the 6R4C model.

*Table 2 Description of the variables in the 6R4C model*

| | **Description** |
|---|---|
| $R_{wo,1}$ | resistance of the inner side of the outer components (outer walls, roof, windows, and door) |
| $R_{wo,2}$ | resistance of the outer side of the outer components |
| $R_{fl,1}$ | resistance of the inner side of the floor |
| $R_{fl,2}$ | resistance of the outer side of the floor |
| $R_{wi}$ | resistance of the inner walls. |
| $R_{vent}$ | thermal resistance for the air exchange with the ambient air due to ventilation, infiltration and thermal bridges |
| $C_z, C_{wi}, C_{wo}, C_{fl}$ | heat capacitances of each temperature node (zone air, inner walls, outer components and floor) |
| $\varphi_{sg}$ | internal solar gain coming through the windows |
| $\varphi_{HP}$ | heat gain from the heating system |
| $s_z, s_{wi}, s_{wo}, s_{fl}$ | distribution factors of internal solar gain for each temperature node |
| $f_z, f_{wi}, f_{wo}, f_{fl}$ | distribution factors of heat gain from the heating system for each temperature node |

In order to consider the external heat exchanges with the outside environments, three temperatures are used as input data. The ambient temperature $T_a$ is related to the effects of ventilation systems and infiltration, which cause heat losses through $R_{vent}$ based on the heat capacity of the zone air and the air change rates for ventilation and infiltration (Nielsen (2005)). The resistance for thermal bridges is calculated from $U_{thermal\ bridge}$ and is included in $R_{vent}$. The short-wave radiation from the sun absorbed by the external surfaces of the building components is considered by introducing a modified equivalent ambient temperature $T_{a,eq}$ as Equation (10) describes, where $I_{dir,v}$ and $I_{diff,v}$ stand for direct and diffuse radiation on the v-th external surface[W/m2], $a_F$ is short-wave absorption [-] and $\alpha_A$ is heat transfer coefficients [W/m²K]. Meanwhile, the external long-wave radiation exchange is neglected due to its small influence as well as the long-wave radiation exchanges among internal surfaces.

$$\boldsymbol{T_{a,eq} = T_a + \sum_v \left[ \frac{U_v A_v}{\sum_v U_v A_v} (I_{dir,v} + I_{diff,v}) \frac{a_F}{\alpha_A} \right]} \quad (10)$$


ISBN 978-2-921145-88-6

$$\dot{T}_z = \frac{1}{R_{vent}C_z}(T_a - T_z) + \frac{1}{R_{wi}C_z}(T_{wi} - T_z) + \frac{1}{R_{wo,1}C_z}(T_{wo} - T_z) + \frac{1}{R_{fl,1}C_z}(T_{fl} - T_z) + \frac{s_z}{C_z}\varphi_{sg} + \frac{f_z}{C_z}\varphi_{HP} \quad (11)$$

$$\dot{T}_{wi} = \frac{1}{R_{wi}C_{wi}}(T_z - T_{wi}) + \frac{s_{wi}}{C_{wi}}\varphi_{sg} + \frac{f_{wi}}{C_{wi}}\varphi_{HP} \quad (12)$$

$$\dot{T}_{wo} = \frac{1}{R_{wo,2}C_{wo}}(T_{a,eq} - T_{wo}) + \frac{1}{R_{wo,1}C_{wo}}(T_z - T_{wo}) + \frac{s_{wo}}{C_{wo}}\varphi_{sg} + \frac{f_{wo}}{C_{wo}}\varphi_{HP} \quad (13)$$

$$\dot{T}_{fl} = \frac{1}{R_{fl,2}C_{fl}}(T_g - T_{fl}) + \frac{1}{R_{fl,1}C_{fl}}(T_z - T_{fl}) + \frac{s_{fl}}{C_{fl}}\varphi_{sg} + \frac{f_{fl}}{C_{fl}}\varphi_{HP} \quad (14)$$

The ground temperature $T_g$ is assumed to be 10 °C and the conductive heat exchange with the floor occurs through $R_{fl,2}$.

As a result, the above considerations lead to four equations of states as described in Equations (11) to (14). Furthermore, these differential equations are discretized and linearized to deal with the sampled data.

# REFERENCE MODELS

## EnergyPlus

The reference models are created in the thermal simulation program EnergyPlus. This program is able to compute detailed temperature trajectories and a building's energy consumption supplied by different heating systems.

## Building model

The geometry of the reference model refers to the same geometric properties as the RC model for comparability.

EnergyPlus can consider natural ventilation by means of a user defined design flow rate. For building type J, which has only natural ventilation, the air change rate is required and set at 0.5 1/h. On the other hand, mechanical ventilation requires a large amount of input data because it is accompanied by a whole HVAC system. Since the main purpose of this study is to evaluate the effects of the heating system, we attempt to simplify a model of mechanical ventilation. The heat losses due to ventilation and infiltration are calculated as follows according to Nielsen (2005).

$$Q = c_{air}V_{zone}\left(\eta_{vent} + \eta_{inf} + \eta_{mec}(1 - \varepsilon)\right) \cdot (T_a - T_z), \quad (15)$$

where $c_{air}$ is the volumetric specific heat of air [J/m$^3$K], $V_{zone}$ is the volume of the zone air [m$^3$], $\eta$ are the change rates for natural ventilation, infiltration and mechanical ventilation [1/h] and $\varepsilon$ is the efficiency of heat recovery of a mechanical ventilation system [-]. Equation (15) implies that the heat loss due to mechanical ventilation can be described by an equivalent change rate for natural ventilation. For example, the heat loss Q with $\eta_{vent}$ of 0.088 is equal to Q with $\eta_{mec}$ of 0.55 and $\varepsilon$ of 0.84. Thus for simplicity, building type L is assumed to have a natural ventilation with the air change rate of 0.088 instead of an explicit model for a mechanical ventilation system.

Modelling thermal bridges requires an additional effort because their effects cannot be simulated separately in EnergyPlus. For instance, the heat losses due to thermal bridges corresponding to $U_{thermal\ bridge}$ can be considered indirectly by changing the properties of all the components that adjacent to the outside air (Lindauer (2017)). In this paper, the thickness of the insulating layer, which has the lowest U-value, is adapted so that the total U-value of the component increases by $U_{thermal\ bridge}$.

Coefficients for convective and radiative heat transfer are based on the following previous studies and standards. An external convective coefficient of 20 W/(m²K) and an internal convective coefficient of 2.7 W/(m²K) are widely adopted. The short-wave absorption coefficient is assumed to be 0.5 as suggested by Harb et al. (2016). The emissivity of long-wave radiation is set at 0.9 by following the default value in EnergyPlus. These values are also used in the RC model for comparability.

## Heating systems

An underfloor heating system with an air-to-water heat pump is considered in this study for two reasons. The first reason is that an underfloor heating system is often accompanied by a heat pump in western Europe (Huang et al. (2015)). Such systems provide flexibility to integrate excess electricity generation from renewable energy sources by DSM. The RC models will finally be applied in this context. Secondly, in case of an underfloor heating system, due to low operating temperatures, the share of the radiant heat transfer is higher than that of the convective heat transfer (Ingenieurbüro für Haustechnik Schreiner (2011)). Radiant heat transfer is associated with temperature difference to the fourth power. Hence, the linearized RC models must be investigated regarding modelling errors arising from the approximations of the nonlinear radiative processes. Hence, we assume that all


ISBN 978-2-921145-88-6

houses considered in the study are equipped with the underfloor heating systems.

The comparative study in this paper focuses on the heat loads transferred to the floor, which are supplied by EnergyPlus in the form of output *RADIANT FLOOR:Zone Radiant HVAC Heating Rate*. The performance of the heating system like the coefficient of performance (COP) of the heat pump is assumed to be independent of the ambient environments here, but will be relevant for future investigations. The heat loads $\varphi_{HP}$ describe the power needed to keep $T_z$ above the minimum temperature required to maintain comfort. The reference temperature is set at a constant value of 19 °C in the field Heating Control Temperature Schedule (name of the EnergyPlus object *ZoneHVAC:LowTemperatureRadiant:VariableFlow).*

## SIMULATION

The aim of this paper is to examine the accuracy of modelling method described in the previous sections. The building model without any heating system is analysed as a first step. We focus on convective and conductive heat transfer first, and then we subsequently examine solar radiation and ventilation including the effects of thermal bridges. In a second analysis, the underfloor heating system is added to the building model.

### Convection and conduction

In this section, the thermal behaviour of a building is analysed by removing the effects of solar radiation, the heating systems and ventilation. This comparison allows to evaluate the thermal behaviour only dependent on the convective and conductive heat transfer between ambient temperature $T_a$ and the building. The sampling time of 15 minutes and the simulation period from 14th February to 28th February are selected in this paper. The zone temperature $T_z$ is calculated in both building type J and L as displayed in Figure 3. The red lines show the results of the RC models for Type J and Type L. The blue lines show the results of the reference models, which are abbreviated to Ref in figures. In addition, weather data such as $T_a$ and $I$ are shown in the figure. The results match well between the RC model and the reference model, indicating that the linear equations in the RC model can well describe convective and conductive heat transfer.

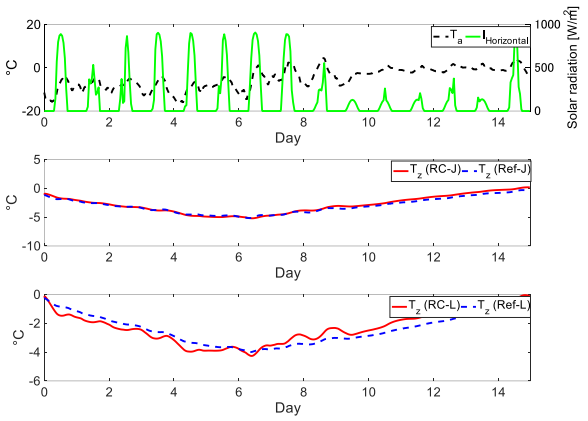


*Figure 3 Zone temperature $T_z$ without solar gains*

### Solar radiation

Figure 4 shows the zone temperatures in the models with solar radiation. The RC model estimates a higher zone temperature than the reference model, especially during the daytime, when temperature rises, in Type L. Given that the temperature rise is driven mainly by solar radiation, the difference between the two models can be attributed to the modelling approach for solar gains in the RC model.

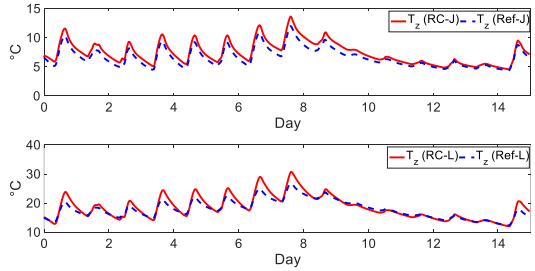


*Figure 4 Zone temperature $T_z$ with solar gains*

In the RC model, the internal solar gain entering through the windows is divided and absorbed by the zone air, the outer components, the inner walls and the floor according to four distribution factors $s_z, s_{wi}, s_{wo}$ and $s_{fl}$ respectively. Factor $s_z$ represents the convective share of the zone air and is well defined in the standard ISO 13790 (2008). On the other hand, the factors $s_{wi}, s_{wo}$ and $s_{fl}$ are determined based on area-weighted averages. In addition, the total internal solar gain $\varphi_{sg}$ [W] is calculated as described in Equation (16) based on direct and diffuse solar radiation, the areas of windows $A_{window,v}$ [m$^2$] and the g-value [-].

$$\boldsymbol{\varphi_{sg} = \sum_v \left[ (I_{dir,v} + I_{diff,v}) \cdot A_{window,v} \cdot g \right]} \qquad (16)$$


ISBN 978-2-921145-88-6

Therefore, the internal gain for each part is assumed to be $s_z\varphi_{sg}$, $s_{wi}\varphi_{sg}$, $s_{wo}\varphi_{sg}$ and $s_{fl}\varphi_{sg}$ respectively.

The differences between the gains in the RC model $s_{wi}\varphi_{sg}$, $s_{wo}\varphi_{sg}$ and $s_{fl}\varphi_{sg}$ and the gains in the reference model $SG_{wi}$, $SG_{wo}$ and $SG_{fl}$ are minimized by curve fitting with the function (17). *Table 3* shows the distribution factors before and after the modification.

$$\min_{s_{wi},s_{wo},s_{fl}} \sum_{t=1}^{T} \left[ \left(s_{wi}\varphi_{sg,t} - SG_{wi,t}\right)^2 + \left(s_{wo}\varphi_{sg,t} - SG_{wo,t}\right)^2 + \left(s_{fl}\varphi_{sg,t} - SG_{fl,t}\right)^2 \right] \quad (17)$$

$$\text{s.t. } s_{wi} + s_{wo} + s_{fl} = 1 - s_z$$

*Table 3 Distribution factors for solar radiation*

| | $s_z$ | $s_{wi}$ | $s_{wo}$ | $s_{fl}$ |
|---|---|---|---|---|
| Area-weighted factors | 0.09 | 0.32 | 0.46 | 0.13 |
| Modified factors | 0.09 | 0.20 | 0.21 | 0.50 |

The zone temperatures are simulated with the modified factors as displayed in Figure 5. The results show that the fitted model has only minor improvements in accuracy of Type J since the unmodified model was already quite accurate. As for Type L, the difference during their peak time is eliminated. The root mean square errors are also calculated in ℃ and the error is reduced from 1.34 ℃ to 0.96 ℃ in Type L.

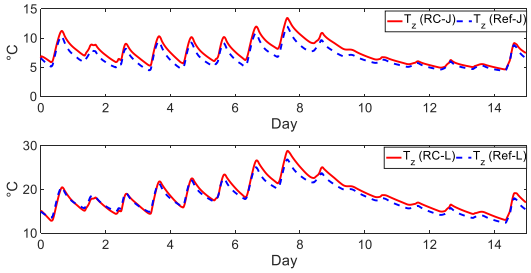


*Figure 5 Zone temperature with modified s factors*

## Ventilation and thermal bridges

The heat losses caused by ventilation and thermal bridges are analysed subsequently. The results are shown in Figure 6 and the only difference between Figure 5 and Figure 6 is whether ventilation and thermal bridges are considered or not. The difference in $T_z$ between the RC models and the reference models in Figure 6 is very small, which is compared to other cases in terms of the root mean square errors (RMSE) in Table 4. This is because the heat losses are in proportion to the difference between the zone temperature and the ambient temperature. Therefore, the RC models, which tend to calculate higher $T_z$, loose a larger amount of heat than the reference models if the heat losses caused by ventilation and thermal bridges are considered.

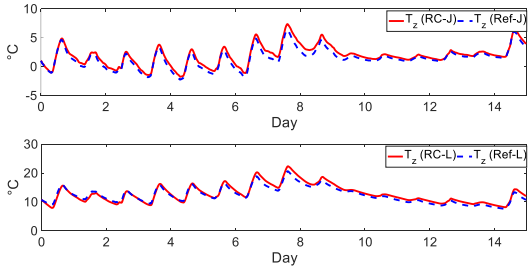


*Figure 6 Zone temperatures with ventilation and thermal bridges*

*Table 4 Modelling error (RSME) of $T_z$*

| Case | Solar radiation | Ventilation and Thermal bridges | RMSE in ℃ Type J | Type L |
|---|---|---|---|---|
| A | No | No | 0.28 | 0.45 |
| B | Yes | No | 0.99 | 0.96 |
| C | Yes | Yes | 0.58 | 0.84 |

## Heating systems

The indicators used for the analysis of the heating system are the zone temperature and the power demand of the heating system.

With regard to the zone temperature, the power demand is simulated in the reference model and then used as input in the RC model. This means that the same power curves are used in both models in order to simulate the zone temperatures. The results are analysed in terms of the RMSE of the zone temperature. Regarding the second indicator, the power demand is simulated in the RC models and the reference models respectively. The RC model calculates the power demand within an optimization, such that $T_z$ is kept higher than 19 ℃ in each current time step, while the reference model refers to the same curves as those used for the first indicator, the zone temperature. The results are analysed in terms of the percentage errors of the total energy demand during the whole simulation period $\sum \varphi_{HP}$, which is obtained by summing up the power demand.

The results of the two comparisons are illustrated in Figure 7 and Figure 8. The zone temperature behavior in the RC models deviates from that in the reference models. In addition, the power demand curves display differences,


ISBN 978-2-921145-88-6

especially the timing and spikiness is relatively weakly reproduced for type L. This indicates the necessity for a modification in the modelling of the heating system.

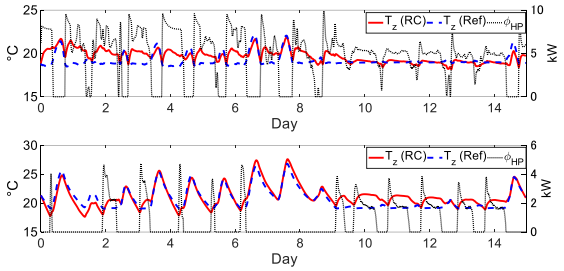


*Figure 7 Zone temperature of the RC model with the area-weighted f factors and the reference model*

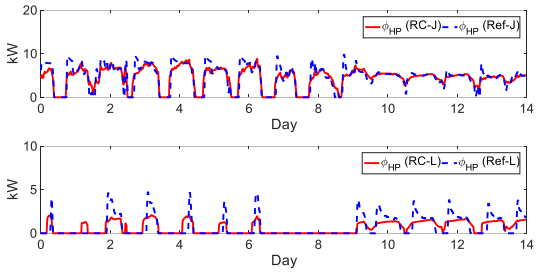


*Figure 8 Power demand curves of the RC model with the area-weighted f factors and the reference model*

In order to model an underfloor heating system, two approaches are considered in this paper. The first approach (approach A) is to modify the distribution factors by using curve fitting in the same manner as done for solar radiation. The optimization in (18) minimizes the squared difference between $T_z$ in the reference and the RC model. Table 5 describes the distribution factors before and after the modification.

$$\min_{f_{wi},f_{wo},f_{fl}} \sum_{t=1}^{T} \left(T_{z,RC} - T_{z,Ref}\right)^2 \qquad (18)$$

s.t. thermal dynamics/RC equations

*Table 5 Distribution factors for underfloor heating systems*

| | $f_z$ | $f_{wi}$ | $f_{wo}$ | $f_{fl}$ |
|---|---|---|---|---|
| Area-weighted factors | 0.05 | 0.39 | 0.39 | 0.17 |
| Modified factors (Type J/L) | 0.05/ 0.05 | 0.05/ 0.04 | 0.46/ 0.43 | 0.44/ 0.47 |

The second approach (approach B) is to introduce an additional thermal resistance $R_{radAW/IW}$ to represent the long-wave radiation. This study focuses on the heat exchange between the outer components and the floor as shown in Figure 9. $R_{radAW/FL}$ is calculated as $1/(\alpha_{str} \cdot A_{FL})$ with a radiant heat transfer coefficient $\alpha_{str} = 5$ W/m²K and the area of the floor $A_{FL}$ [m²] based on the VDI 6007. In this approach, the whole amount of the heat gain is added to the floor's.temperature node.

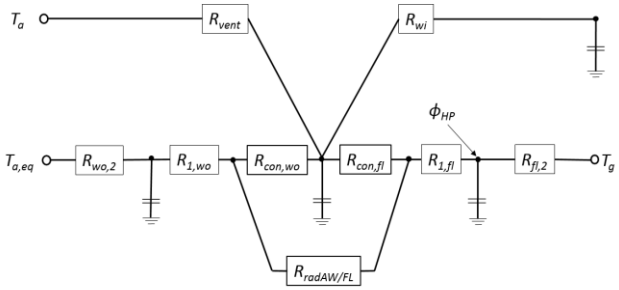


*Figure 9 Model structure with an additional thermal resistance*

The results of the zone temperature and the power demand simulated with the approach A or B are shown in Figure 10 to Figure 13, indicating that both the approach A and B improve the accuracy of the RC model.

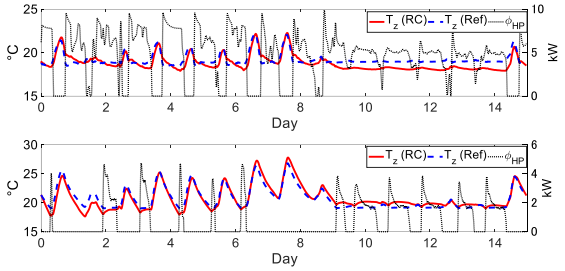


*Figure 10 Zone temperature of the RC model with the approach A and the reference model*

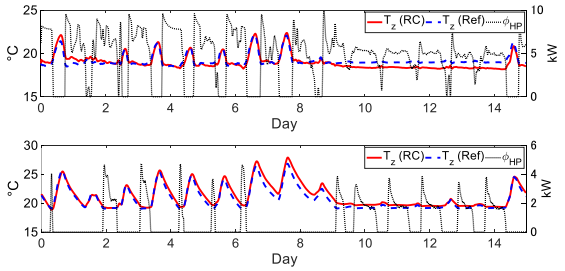


*Figure 11 Zone temperature of the RC model with the approach B and the reference model*


ISBN 978-2-921145-88-6

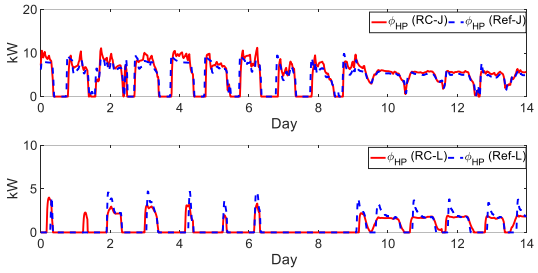


*Figure 12 Power demand curves of the RC model with the approach A and the reference model*

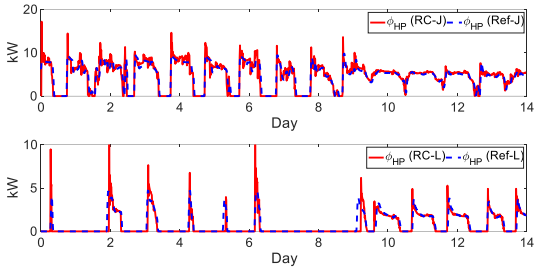


*Figure 13 Power demand curves of the RC model with the approach B and the reference model*

Since parameter fitting used for the approach A is conducted by using the data during the period from 14th February to 28th February as a target, the robustness of the fitted parameters should be examined. Hence, we change the time interval and carry out simulations with the same fitted parameters. The RMSE of the zone temperature are obtained as Table 6 describes. Because the errors are not significantly different in the different time interval, this paper concludes that the model with the fitted parameters has high robustness against different time intervals.

*Table 6 Modelling error (RSME) of $T_z$ during different time intervals*

| Period | First date | Second date | RMSE in °C | |
|---|---|---|---|---|
| | | | Type K | Type L |
| ( I ) | 1st Jan | 15th Jan | 0.76 | 0.49 |
| ( II ) | 17th Jan | 31th Jan | 0.79 | 0.62 |
| (III) | 1st Feb | 15th Feb | 0.77 | 0.68 |
| (IV) | 14th Feb | 28th Feb | 0.64 | 0.72 |

Lastly, the accuracy of the default model without any modifications (Model Default), the model with the modified f factors (Approach A) and the model with the additional thermal resistance (Approach B) are compared in terms of the RMSE of the zone temperature and the percentage error of the total energy demand as shown in Figure 14. Both approaches A and B reduce the errors in most cases. One exception is the percentage error of the total energy demand in Type J, where the results are relatively similar between the three models because Model Default has also a small error.

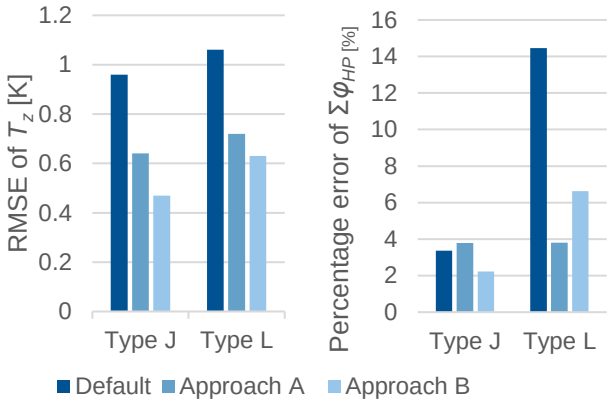


*Figure 14 Errors for $T_z$ and $\sum \varphi_{HP}$*

## CONCLUSION

The main aim of this study is to evaluate the accuracy of a RC building model equipped with an underfloor heating system which is modelled based on the German guideline VDI 6007. A reference model is implemented in EnergyPlus to provide a comparison. In a first step, the study considers the convective and conductive heat transfer between the building and the outside environments, finding that their effects are simulated with high accuracy in the RC model. Subsequently, we examine the radiation heat transfer and the main finding of this study is that an area-weighted approach can be insufficient to model radiation from solar gains and the underfloor heating systems. A higher accuracy is received when a curve fitting approach determines the distribution factors. Afterwards, the modelling method for the underfloor heating system is investigated and two approaches are compared. The first approach is to modify the area-weighted factors by using curve fitting and the second one is to introduce a thermal resistance representing the long-wave radiation. In order to analyse the results, this study uses the RMSE and the percentage errors of the energy demand. Results indicate that both approaches result in an effective improvement of the model's accuracy. The second approach with an


ISBN 978-2-921145-88-6

additional thermal resistance gives in particular better results in most cases.

Further investigation is needed on the analysis of the heating system. In particular, the efficiency of the heat pump will be considered in future work. In addition, other kinds of heating systems require further discussion. For instance, radiators are widely used in residential buildings, while their thermal behaviour and applicability for DSM is different from that of an underfloor heating system.

## ACKNOWLEDGEMENT

The authors would like to thank the Yutaka Takahashi Fellowship from Department of Civil Engineering at the University of Tokyo for the financial support to Ryuta Kuniyoshi.

## REFERENCE

Arold, J. 2014. Perspektiven von Strom zur Wärmeerzeugung in Niedrigstenergiegebäuden. *Doctoral dissertation at University of Stuttgart.*

Beuth Verlag. 2015. Guideline VDI 6007-1.

Harb, H., N. Boyanov, L. Hernandez, R. Streblow, D. Müller. 2016. Development and validation of grey-box models for forecasting thermal response of occupied buildings. *Energy and Buildings 117,* 199-207.

Huang, M. J., N. Hewitt. 2015. The Energy Conservation Potential of Using Phase-Change Materials as Thermal Mass Material for Air Source Heat Pump-Driven Underfloor Heating System in a Building. *Progress in Clean Energy* 2, 209-227.

Ingenieurbüro für Haustechnik Schreiner (IBS). 2011. Wärmeabgabeszsteme - Grundlagen Raumheizsysteme. Retrieved January 21, 2018. From http://energieberatung.ibs-hlk.de/grundl_wasys.htm.

International Standard DIN EN ISO 10456. 2007. Berlin: Beuth Verlag.

International Standard DIN EN ISO 12831. 2012. Berlin: Beuth Verlag.

International Standard DIN EN ISO 13790. 2008. Berlin: Beuth Verlag.

Kramer, M., A. Jambagi, V. Cheng. 2017. Bottom-up Modeling of Residential Heating Systems for Demand Side Management in District Energy System Analysis and Distribution Grid Planning. In 15th *International Building Simulation Conference of IBPSA,* San Francisco, pp. 711-718.

Lauster, M., P. Remmen, M. Fuchs, J. Teichmann, R. Streblow, D. Müller. 2014. Modelling long-wave radiation heat exchange for thermal network building simulations at urban scale using Modelica. *In 10th International ModelicaConference,,* Lund.

Lindauer, M. 2017. Dynamische Sensitivitätsanalyse-methoden energetischer Wohnge-bäudequartiers-simulationen, *Doctoral dissertation at Technical University of Munich*.

T. R. Nielsen. 2005. Simple tool to evaluate energy demand and indoor environment in the early stages of building design. *Solar Energy* 78, 73-83.

Reynders, G., J. Diriken, D. Saelens. 2014. Bottom-up modeling of the Belgian residential building stock: influence of model complexity. In *9th International conference on system simulation in buildings,* Liège.

Reynders, G., J. Diriken, D. Saelens. 2014. Quality of grey-box models and identified parameters as function of the accuracy of input and observation signals. *Energy and Buildings* 82, 263–274.

Tenbohlen, S., M. Brunner, M. Schmidt, T. Henzler. 2015. Be- und Entlastung elektrischer Verteilnetze durch Wärmepumpen bei der Wärmeerzeugung in Wohngebäuden. *University of Stuttgart*.

Zentralverband Elektrotechnik- und Elektronikindustrie e.V. (ZVEI), Bundesverband der Energie- und Wasserwirtschaft e.V. (bdew). 2012. Smart Grids in Germany.


ISBN 978-2-921145-88-6